ENG-48

730069

INDEX NO. BP-139
This document contains 73 pgs, and 13 plates of figures.
This is Copy 2 of 34. Series A

DO NOT REMOVE THIS PAGE

Issued to: R. Loevinger

THIS IS A CLASSIFIED DOCUMENT

RESTRICTED

(Classification to be stamped here)

1. This document contains restricted data within the meaning of the Atomic Energy Act of 1946 and/or information affecting the national defense of the United States within the meaning of the Espionage Act U. S. C. 31 & 32, as amended. Its transmission or the revelation of its contents in any manner to an unauthorized person is prohibited and may result in severe criminal penalty.
2. Before this document can be given to a person to read, his name must be on the Reading List of those authorized to read material on this subject, or permission must be obtained from the Information Division or the Executive Office.
3. A SECRET or CONFIDENTIAL document is to be kept only in a guarded area. When stored, it must be kept in a locked safe or in a locked filing case with a tumbler lock.
4. A SECRET or CONFIDENTIAL document is not to be copied or otherwise duplicated without permission of the originating office. Extensive notes on the contents of a secret report may be taken only in a bound notebook with numbered pages, having the designation SECRET. This must be safeguarded in the same way as a Secret Report (See 1, 2 and 3). Other notes must be avoided, but if made must be done in a form meaningless to anyone but the writer and later destroyed.
5. The person or office to whom a SECRET ot CONFIDENTIAL document is issued is accountable for the document at all times. A system of accountability by signed receipts or a signed record book must always be used. Permission for transmission to another office than that of the assignee must be obtained through the Information Division and recorded there.
6. After a document passes the stage of usefulness to its possessor, it should be returned to the Information Division, whereupon the individual will be relieved of the responsibility for its safe-keeping.
7. Initial and date the pages of this document which describe any work that you have witnessed, adding any pertinent information, such as references to original work records. This document, properly signed, dated and annotated, is important in patent preparation.
8. Each person who reads this document must sign this cover sheet below. Please sign and date the cover sheet after reading the report. Also state by Yes or No whether or not notes have been taken. See paragraph 4 above.

Route to	Read by	Notes?	Date	Route to	Read by	Notes?	Date
	1263226						

CLASSIFICATION CANCELLED OR CHANGED TO Unclassified
BY AUTH. CG-DAR-1
DATE 3/4/96
BY

A-16

University of California

Radiation Laboratory

Department of Physics

Contract No. W-7405-Eng-48

IONIZATION CHAMBER STUDIES OF ENERGY TRANSFER FROM 100 MEV NEUTRONS TO LIGHT NUCLEI

by Robert Loevinger

October 21, 1947

Berkeley, California

ABSTRACT

If an ionization chamber consisting of a small cavity in solid material is placed in a field of non-ionizing radiation, then, under certain conditions, there exists the following relationship:

Energy dissipated per unit volume of wall material =
average energy per ion pair in the gas X relative
stopping power for the ionizing secondaries X number of ion
pairs formed per unit volume in the gas.

This relationship has been known for many years. In order to apply it to the 100 Mev neutron beam, it has been formulated in a sufficiently general fashion so that it can be used without detailed knowledge of the nature of the interaction between the neutrons and the nuclei.

In order to determine the conditions under which the stated relationship is valid for the 100 Mev neutron beam, the ionization has been studied as a function of size of cavity, thickness of wall material, and composition of wall material. The effects of neutron attenuation and backscatter have been determined. The result is a determination of the relative contribution of hydrogen, carbon, and oxygen nuclei to the total energy dissipation in hydrogenous solids. The measurements also yield a determination of the absolute value of the energy flux of the neutron beam, which checks closely with a simultaneous determination made by an entirely different method.

The results can be used to calculate the energy dosage to tissue of known composition from a monitored exposure to the neutron beam, with an accuracy of about 10%. The results will also be useful in the future in developing the theory of the interaction between 100 Mev neutrons and the light nuclei, particularly with regard to star formation.

TABLE OF CONTENTS

I - Introduction

This paper presents information secured regarding the interaction of 100 MEV neutrons with light nuclei, by ionization chamber studies. The central problem is the computation of the energy transferred from the neutron beam to an arbitrary solid composed of hydrogen, carbon, and oxygen, that is to say, the determination of the tissue energy dose.

When the ionization chamber is to be used to study the properties of a radiation field, there are in general two types of chamber which may be used: If the chamber is sufficiently large, so that when placed in an external radiation field the secondary particles from the walls make a negligible contribution to the observed ionization then the ionization depends only upon the radiation, and the pressure and composition of the gas in the chamber. If the chamber, on the other hand, is sufficiently small so that the observed ionization is due only to the secondary particles from the walls, the contribution from the secondaries arising in the gas being negligible, then there is a simple relationship between the radiation, the pressure and composition of the gas, and the properties of the walls. An ion chamber of intermediate size presents in general a much more difficult problem in the analysis of the observed ionization. Since a 10 Mev proton has a range of about 1 meter in air, and a 100 Mev proton has a range of 70 meters in air, it is clear that the small chamber is the appropriate one for the present study.

The general approach is indicated by the Table of Contents. Section II is a critical examination of the relationship between the incident flux, the properties of the gas and the wall material, and

the observed ionization in a cavity chamber. This section is quite general in its language and application, applying to any non-ionizing radiation flux (neutrons or photons). Section III consists of a discussion of the special form which this relationship takes when applied to the present case, and an evaluation of the constants needed. Sections IV and V present and discuss the experimental applications to the neutron beam.

II - The Bragg-Gray equation.

1. Origin of the Equation.

The first quantitative discussion, known to the writer, of the relationship between the observed ionization and the processes taking place in the walls of the ion chamber was made by Sir William Bragg in 1912[1]. He was investigating the ranges of the recoil electrons resulting from gamma rays. That part of his argument which concerns us here may be stated as follows: Consider a substance uniformly irradiated by gamma rays. The total length of the tracks of the recoil electrons crossing a small volume of arbitrary shape inside the substance is proportional to the product of the intensity of the gamma radiation, the mass coefficient of absorption of the gammas, and the range of the secondary electrons. This product is independent of density, uniformity of material, and crookedness of the electron tracks. The range in question need not be the same for all the particles, but is an average. Suppose now that the small volume in question is a vacuum. This will not change the distribution of the electrons in its neighborhood, since any electron crossing the cavity will not have its range in matter (measured, say, in mg./cm^2) changed in amount or direction. Hence, the total length of the paths of the electrons crossing the cavity is the same as for a similar volume of wall material situated nearby. If now we introduce air into the cavity, this conclusion will not be changed, provided the cavity is not too large, nor the pressure too high. The extent to which this last conclusion is valid may be tested, Bragg suggests, by measuring ionization as a function of pressure. If the relationship is linear, the cavity does not affect the number of electrons crossing

it.

From this argument, we can at once write down, in modern terminology, the desired relationship. For

$$\text{length of path in unit volume} = \frac{E_w}{\left(\frac{dE}{dx}\right)_w} = \frac{E_a}{\left(\frac{dE}{dx}\right)_a}$$

where E_w and E_a are the energies dissipated per unit volume in the wall and in the air of the cavity, respectively, by the electrons losing energy at the rate $\left(\frac{dE}{dx}\right)$, with the appropriate subscript. So then

$$(1) \qquad E_a = WN_v = \frac{1}{S} E_w$$

where N_v is the number of ion pairs /cc/sec formed in the cavity, W is the average energy per ion pair in air, and S is the stopping power of the wall material for electrons relative to air. This then is the desired relationship, which we shall refer to as the Bragg-Gray equation. It was first stated in the quantitative form of Eq. (1) by L. H. Gray[2] in 1929, as part of a cosmic ray investigation, who deduced it independently. His proof consisted in showing first, by mathematical induction, that the distribution of the electrons is not disturbed in the neighborhood of the cavity, and then showing by a rather elaborate geometrical argument that our Eq.(1) followed from this fact. His statement of the equation, and his formulation of the conditions under which it is valid, are quite correct provided that his main assumption is justified, namely, that ~~the relative stopping power~~ W and S is independent of energy. However, his manner of proof adds but little physical insight, so that it will not be repeated here.

A third derivation of the Bragg-Gray equation was contributed by G. C. Laurence [3] in 1937, who was discussing the measurement of the intensity of X-rays with energies above 500 kv. His very ingenious approach to the problem is the basis of the detailed discussion of the next section. The derivation of the Bragg-Gray equation given there differs from that given by Laurence only in that it is somewhat more general in its formulation, and it is in terms of the conventional functions used by modern physics. Laurence's rather complicated [redacted] result, which is in reality Eq.(1) in its most general form, will be shown to be capable of quite a simple formulation, without loss of generality.

The transfer of energy from the primary, non-ionizing radiation to the wall material takes place in two steps. First, ionizing secondary particles are created by elastic or inelastic collisions between the primary particles and the atoms of the walls, and these ionizing particles then dissipate their energy by ionization and excitation of the atoms near which they pass. As a result, if we consider a region in the wall material sufficiently far from the outer boundaries so that the primary radiation is in equilibrium with its secondaries, the energy dissipated per cc. can be expressed as

$$(2) \qquad E_w = \sum_i^{n_i} \not{M}_i \int_0^{\infty} IE\, \gamma_i\, k_i\, \sigma_i \, dE$$

where n_i is the number of atoms per cc of type i , IdE is the primary flux in particles/cm^2/sec between E and E + dE, γ_i is the average energy of a secondary in a type i collision expressed as a fraction of the energy of the primary particle, k_i is the average number of ionizing secondaries created in a type i collision, and σ_i is the

collision cross section of type i atoms for the production of one or more ionizing particles. From this it follows at once that Eq. (1) can be written in the explicit form

$$N = \frac{V}{SW} \Phi \sum_i n_i \overline{\gamma_i k_i \sigma_i} \tag{3}$$

where N is the number of ions formed per second in the cavity, V is the volume of the cavity, $\Phi = \int_0^\infty IEdE$ is the primary energy flux, and the bar signifies "average over the primary energy spectrum weighted with the energy".

Eq.(3) is essentially the form of the Bragg-Gray equation which is applied in the present investigation to the neutron beam from the 184-inch cyclotron. In the next section it is derived in a somewhat more general form.

2 - Detailed Cavity Theory

Consider a cavity of arbitrary shape in a solid material in a radiation field. Suppose this to be non-ionizing radiation (neutrons or photons). If the cavity is filled with air or some other gas, ionization will appear in it, and under suitable conditions this can be measured. We seek the relationship between the ionization in the cavity, the incident radiation flux, and the properties of the gas and the solid.

Suppose first that the radiation is monoenergetic, and parallel to some fixed direction, say $\theta = 0$. Then the number of ionizing particles created per second in volume element dx dy dz at the origin, with energy between E_1 and $E_1 + dE_1$, and which travel in a direction lying within the solid angle $d\omega$, is just

$$d\eta = I n \sigma^- f(\Theta, E_1) \frac{d\omega}{4\pi} dE_1 \quad dxdydz$$

where I is the flux of primary radiation in particles/cm^2/sec, n is the number of atoms/cc in the wall material assumed to be a single element only, σ^- is the cross section for collision with production of ionizing particles, $d\omega = \sin\Theta \, d\Theta \, d\phi$, and $f(\Theta, E_1) \, d\omega \, dE_1$ is the probability that an ionizing particle created in the volume element dx dy dz, will have an energy in the range $E_1 + dE_1$, and a direction within the solid angle $d\omega$.

Assume first that the ionizing secondary particles reach the cavity without deflection in the wall material. Suppose further that the dimensions of the cavity are so small compared to the range in the gas of the cavity of the ionizing particles, that the change in energy of the particles in crossing the cavity can be neglected in considering the stopping power of the gas. Then the number of ion pairs created in the cavity per second, by the $d\eta$ particles, due to energy dissipated through ionization and excitation, is

$$(4) \qquad dN_1 = \frac{S_a(E_2)}{W(E_2)} \quad t \quad d\eta$$ See diagram, page 11.

where $W(E_2)$ is the average energy per ion pair in the gas of the cavity for ions created by the ionizing particles, S_a is the stopping power (energy loss per cm. taken as a positive number) in the gas (air) of the cavity, t is the distance across the cavity, and E_2 is the energy of an ionizing particle when it reaches the edge of the cavity.

Then the number of ion pairs created per second by all those

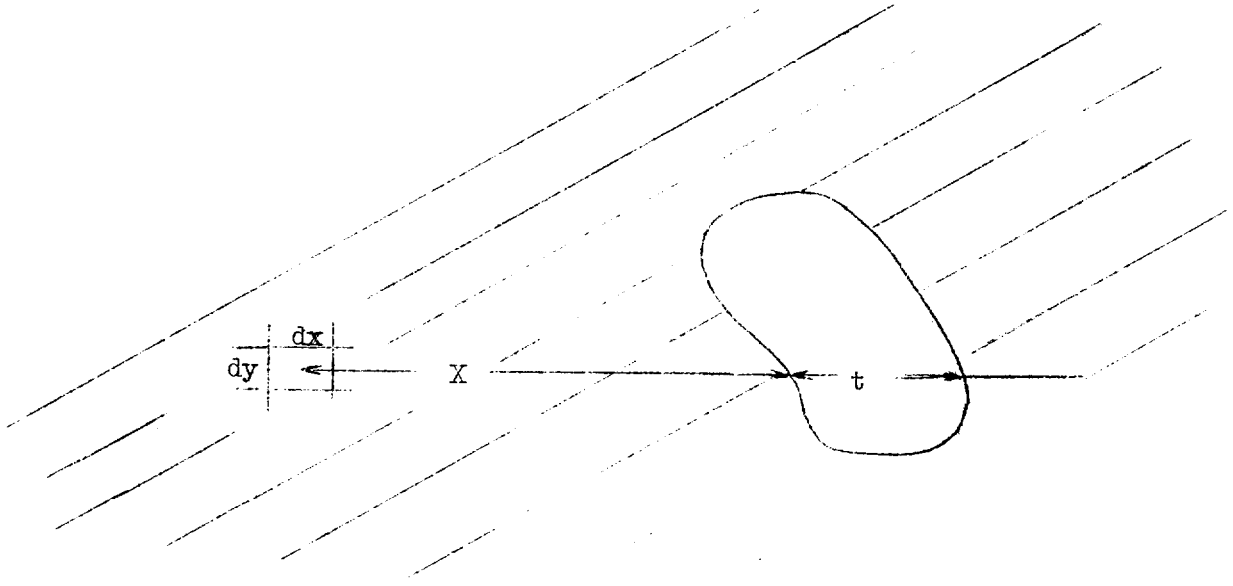

Illustration for Equation (4)

secondaries created at energy E_1 and thereafter travelling in the positive x-direction, is just

$$(5) \qquad dN_2 = I \eta \sigma f(\theta, E_1) \, d\omega \, dE_1 \iiint t \, \frac{S_a}{W} \, dx \, dy \, dz$$

The integral is $\int_{-\infty}^{+\infty} dz \int_{-\infty}^{+\infty} dy \int_{x_o - r}^{x_o} dx \; t(y,z) \; \frac{S_a(E_2)}{W(E_2)}$

where x_o = x-coordinate of the cavity surface, and r = range in the wall material of the ionizing secondaries. Since the ionizing particle is created at x with initial energy E,

$$E_2 = E_1 - \int_0^{x_o - x} S_w (E_1, x') \, dx'$$

$$\text{So} \qquad dE_2 = \frac{\partial E_2}{\partial (x_o - x)} \, \frac{\partial (x_o - x)}{\partial x} \, dx = S_w(E_1, x_o - x) \, dx = S_w (E_2) \, dx$$

where S_w is the stopping of the wall material for the ionizing secondaries. So now the integral becomes

$$\int_{-\infty}^{+\infty} dz \int_{-\infty}^{+\infty} dy \int_0^{E_1} dE_2 \; \frac{t(y,z)}{W(E_2)} \; \frac{S_a(E_2)}{S_w (E_2)} = V \int_0^{E_1} \frac{1}{W} \, \frac{Sa}{Sw} \, dE_2$$

where V is the volume of the cavity. So now

$$(5') \qquad dN_2 = V I \eta \sigma f(\theta, E_1) d\omega dE_1 \int_0^{E_1} \frac{1}{W} \, \frac{Sa}{S_w} \, dE_2$$

Let now $f(E_1)dE_1 = dE_1 \iint f(\theta, E_1) \sin \theta \, d\theta \, d\phi$ = the probability than an ionizing secondary be created in the energy range E_1 to $E_1 + dE_1$. Then the number of ion pairs created per second in the cavity by secondaries created with initial energies in

the range E_1 to $E_1\ dE_1$, and travelling thereafter in any direction whatsoever, is just,

$$(6) \qquad dN_3 = V\eta\sigma\, f(E_1)\, dE_1 \int_0^{E_1} \frac{1}{W}\,\frac{S_a}{S_w}\, dE_2$$

So finally, the total number of ion pairs created per second in the cavity is

$$(7) \qquad N = V\eta\sigma \int_0^{E} f(E_1)\ dE_1 \int_0^{E_1} \frac{1}{W}\ \frac{S_a}{S_w}\ dE_2$$

where E is the energy of the primary particles.

Before proceeding further, let us remove the necessity for the assumption that the ionizing particles are undeflected in the wall material. Suppose that, of the $d\eta$ secondaries, a fraction $\alpha\ da\ d\Omega$ are scattered through an angle ψ into a cone of solid angle $d\Omega$, after travelling a distance a in the original, x-direction. Then Eq. (4) becomes

$$dN_1 = \frac{S_a(E_2)}{W(E_2)}\ t\ d\eta\ (1-\alpha da\, d\Omega) + \frac{S_a(E_2')}{W(E_2')}\ t'\ d\eta\ (\alpha\ da\, d\Omega)$$

See diagram, p. 14

where t' is the distance across the cavity in the new direction, and E'_2 is the energy of the scattered particles on reaching the edge of the cavity. Then, to the triply-iterated integral following equation (5) must be added the two integrals

$$-\alpha\, da\, d\Omega \int dz \int dy \int dx\ \ t\ \frac{S_a(E_2)}{W(E_2)} = -\alpha\, da\, d\Omega\ V \int_0^{E_1} \frac{1}{W}\ \frac{Sa}{S_w}\ dE_2$$

$$+\alpha\, da\, d\Omega \int dz \int dy \int dx\ t'\ \frac{S_a(E'_2)}{W(E'_2)} = \alpha da\, d\Omega \int dz \int dy \cos\psi \int \frac{dx}{\cos\psi}\ t'\ \frac{S_a}{W}$$

$$= \alpha da\, d\Omega\ V \int_0^{E_1} \frac{1}{W}\ \frac{S_a}{S_w}\ dE'_2$$

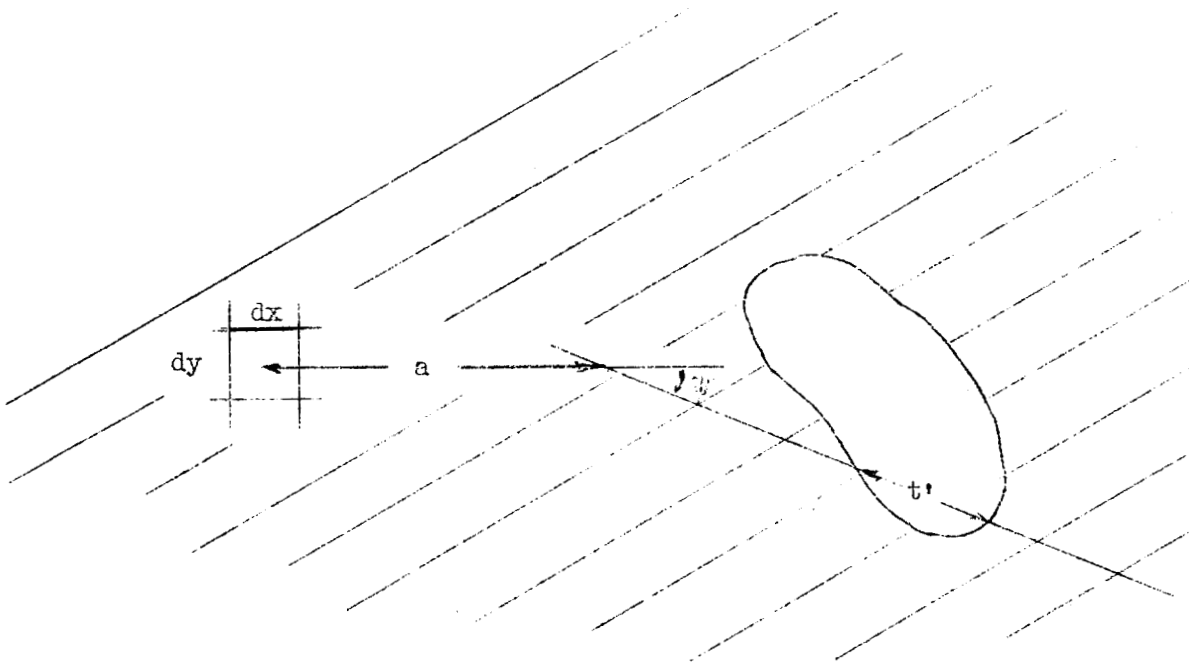

Illustration for Equation (7)

These two integrals are equal, so that single scattering leaves the ionization in the cavity unchanged. The argument is at once generalized to multiple scattering, giving the conclusion that Eq. (7) is unchanged by scattering in the wall material.

Eq. (7) applies to a monoenergetic radiation field incident on a solid containing a single type of atom, where the collision process produces a single ionizing secondary. For the most general case, the corresponding result can be written down by inspection, in the form

$$N = V \sum_i \int_0^{\infty} dE\ I(E)\,\sigma_i(E)\,k_i(E) \int_0^{E} dE_1\ f_i(E_1) \int_0^{E_1} \frac{1}{W_i(E_2)} \left(\frac{S_a(E_2)}{S_w(E_2)}\right)_i dE_2 \tag{8}$$

where $I(E)dE$ is the incident particle flux in the energy interval $E + dE$, i is a subscript distinguishing the several types of atoms in the wall material and the possible types of collision with each, and k_i is the average number of ionizing particles produced in a type i collision.

Now $S = S_w/S_a$ is a standard function, the relative stopping power. Let

$$R_i(E_1) = \frac{1}{E_1} \int_0^{E_1} \frac{dE_2}{W_i S_i} \tag{9}$$

R_i is just the mean value of the function $1 / W_i S_i$, averaged over all energies from zero up to E_1. Then let

$$P_i(E) = \frac{\int_0^{E} E_1\, f_i(E_1)\, R_i(E_1)\, dE_1}{\int_0^{E} E_1\, f_i(E_1)\, dE_1} \tag{10}$$

P_i is the mean value of R_i for all the ionizing particles produced

by a primary of energy E in a type i collision. Then let

$$(11) \qquad \gamma_i = \frac{1}{E} \int_0^E E_1 \; f_i(E_1) \; dE_1$$

γ_i is evidently the average energy of a secondary particle in a type i collision, expressed as a fraction of the energy of the primary particle. Now equation (8) can be written

$$N = V \sum_i \eta_i \int_0^\infty dE \; I \; \sigma_i \; k_i \; \gamma_i \; P_i$$

This can then be written in the simplified form

$$(12) \qquad N = V \; \Phi \sum_i \eta_i \; \overline{P_i \; \gamma_i \; k_i \; \sigma_i}$$

where $\Phi = \int_0^\infty EI(E) \; dE$ is the primary energy flux. The bar signifies "average over the primary energy spectrum weighted with the primary energy".

Eq. (12) is the desired relationship between observed ionization in the cavity, the primary flux, and the properties of the gas and the wall material. This result could have been reached by a much simpler argument, in the following manner: Accepting the proofs of Gray and Bragg, as demonstrating Eq.(3), we must still allow for an energy dependence of W and S. Taking Equation (1) as valid for a given particle energy, we first form an average to take account of the fact that particles created at a given energy arrive at the cavity with all energies between zero and the initial energy. This corresponds to Equation (9). Then we take another average, corresponding to Eq. (10), to take into account the energy spread in the secondaries created by a given primary. Then a third average, taking

account of the energy spread of the primary radiation and the number of secondaries per collision, gives just Equation (12). Thus the present rather elaborate derivation contributes only a detailed understanding of the limitations of the final equation, rather than any quantitative, new result. However, for those circumstances where the dependence upon energy of relative stopping power or energy per ion pair is important and can be determined, Equation (12) presents the possibility of a somewhat more accurate analysis of certain types of ion chamber measurements than has thus far been attempted, with the exception of the work of Laurence [3].

An examination of the discussion of this section will show that the following conditions are explicitly or implicitly laid down for the validity of Equation (12):

1 - The dimensions of the cavity must be somewhat less than the minimum range in the cavity of the ionizing particles arising in the walls.

2 - The wall thickness must be at least as great as the maximum range of the ionizing particles in the wall material.

3 - The variation in intensity of the primary radiation over the region from which ionizing particles reach the cavity must be negligible.

4 - The ionization due to secondaries created in the gas of the cavity must be negligible compared to ionization due to secondaries created in the walls.

5 - Scattering of the ionizing particles in the gas of the cavity can be neglected.

These five conditions will be referred to as the "cavity condi-

tions" and an ion chamber which meets them, as a "cavity chamber". The requirements imposed by these cavity conditions form a large part of the subsequent discussion, and of the experimental work.

It was tacitly assumed that the wall material was uniform in density. This is not required, for if all distances were measured in, say, mg./cm^2 instead of cms., the proof would go through unchanged Thus the result is valid for walls not uniform in density. In fact, the ionization in a cavity chamber is independent of wall density altogether, since it cancels out between P_i and n_i . This result, perhaps at first sight surprising, is a result of the second of the cavity conditions cited above.

While the derivation started with the specification that the primary radiation be parallel, the result is independent of all angular variables and of the shape of the cavity. Thus the ionization in a cavity chamber is independent of the direction of the primary radiation.

It is perhaps worth pointing out that, contrary to statements frequently encountered in discussions of radiation dosimetry, no assumption is made in arriving at Equation (12) or its simpler equivalent Eq. (3), concerning the energy per ion pair in the wall material. This quantity enters only when considering ionization in the wall material. While this is certainly a matter of considerable importance in studying the biological effects of radiation, it will not be considered further in the present investigation.

3. - Verification of the Bragg-Gray equation

If the relative stopping power and the average energy per ion pair are independent of energy, the general form Eq.(12), reduces at once to Eq.(3):

$$N = \frac{V}{SW} \Phi \sum_i \frac{n_i}{M_i} \overline{\nu_i \; k_i \; \epsilon_i} \qquad (3)$$

In this form the relationship has been extensively tested. Gray 4) first made a critical examination of the relationship, in discussing the absolute determination of gamma-ray energy. First Gray shows that the average energy per ion pair, W, and the relative stopping power, S, for the secondary electrons from gamma-rays are constant with sufficient accuracy for purposes of application of Eq. (3). He then points out that "the equation requires (1) that the ionization per unit volume should be independent of the size of the chamber; (2) that the ionization in a given chamber should be proportional to the gas pressure; (3) that the ionization in different chambers should be proportional to the gamma-ray energy absorbed per unit volume of the wall material, and inversely as its stopping power". By a very careful series of measurements on chambers of different sizes and different materials, filled with air at various pressures between 10 and 74 cms., he shows that the observations satisfy these three requirements within a few percent in all cases, and indicate the basic validity of the relationship in question.

Aebersold and Anslow 6) in connection with a very extensive series of measurements on the 5 Mev neutron beam of the 37-inch Berkeley cyclotron, measured gamma-ray ionization as a function of pressure, from about 10 cms. to 76 cms., for some 16 different gases. These measurements were made with a filtered Ra source. For all the gases the ionization was accurately linear with pressure over the region observed. From the relative ionization in the different gases, they computed

stopping powers by means of the Bragg-Gray equation, and got values in close agreement with alpha-particle stopping powers found by other observers. Similar measurements with air-filled thimble chambers made of some seven different materials, exposed to gamma radiation, gave again ionization linear with pressure from a few cms. up to 80 cms. When they used these same thimble chambers in the neutron beam, they found the linear relationship to hold only when the pressure was sufficiently low so that the secondary particles from the wall completely crossed the chamber. The transition pressures, at which the cavity conditions are no longer satisfied, are clearly visible on many of their curves.

The most extensive application and verification of the Bragg-Gray equation has been in connection with investigations of the medical problem of X-ray and gamma-ray dosimetry. A summary of the work in this field through 1939, giving references to the many original papers, is contained in the review article by Kaye, Bell, Binks, and Perry [11]. A more recent summary is given in some of the articles in the reference volume entitled Medical Physics [10]. While the work reported in these articles is concerned primarily with determining actual tissue doses, the extrapolation chamber developed by Failla for accomplishing this furnishes a very valuable means of verifying the Bragg-Gray equation. The extrapolation chamber, described in detail in the last two references, is simply a parallel-plate ionization chamber so designed that the spacing between the plates can be varied within wide limits. If then the ionization per unit volume is determined as a function of the plate spacing, it will be found to approach a limiting value independent of plate spacing as the plate spacing is decreased. This again is just the behavior predicted by the Bragg-Gray equation.

Thus it is reasonable to consider that the Bragg-Gray equation has been verified, and can be accepted without reservations. The problem in applying it is the determination of the exact conditions under which it is valid for a

particular radiation field. Under some circumstances it would be difficult or impossible to construct an ion chamber meeting the cavity conditions with any accuracy.

The first two of the cavity conditions cited, [redacted], relating to the dimensions of the cavity and the thickness of the walls, are to be considered as experimental requirements to be examined separately for each radiation field. The third, having to do with the variation in the intensity of the primary radiation in the neighborhood of the cavity, will normally be a correction to be applied to the observed ionization. The last two, relating to the contribution to the observed ionization by the gas of the cavity, can be considered as satisfied by any experimental set-up where the observed ionization per unit volume is either linear with pressure from the operating pressure down to zero, or independent of the size of the ion chamber from the operating size down to zero. This last statement is due to the fact that the ionization per unit volume (or the energy dissipated per unit volume) due to collisions between the primary radiation and the gas of the cavity, is not given by an expression of the form of Eq. (2), but is proportional to the stopping power of the gas itself, and to an average dimension of the cavity, and thus must go to zero with either of these quantities. Likewise scattering by the gas of the cavity of secondaries originating in the walls must approach zero for the limiting case of either zero volume or zero gas.

III - Application of the Cavity Chamber to the 100 MEV Neutron Beam.

1. - General Equations

The problem of the determination of the energy transfer from a neutron beam to an hydrogenous solid was discussed in great detail by Gray [5] in 1944. His equation is equivalent to Eq. (3) of the present discussion, provided that for the fractional energy transfer from a neutron to a nuclear secondary particle we can use the value appropriate to an elastic collision isotropic in the center of mass coordinates, that is, in the present notation,

$$\gamma_i k_i = \frac{2A_i}{(1+A_i)^2} \tag{13}$$

where A_i is the atomic weight of the recoiling atom. As Gray points out, this is certainly a reasonable assumption for hydrogen recoils up to 10 Mev or so, and need be only approximately true for other light nuclei, since most of the energy transferred to an hydrogenous solid will be due to hydrogen recoils for neutron energies below 10 Mev. For a reasonably monoenergetic neutron beam with energy of a few Mev, his very lucid and detailed discussion of the accuracy of this method of determining energy transfer from neutrons is certainly valid. But if the beam of neutrons has a wide energy spectrum, and particularly if there are many neutrons below a few Mev, the accuracy of the simple Eq. (3) will be much less, since in that energy region both the relative stopping power for protons, and the collision cross section for hydrogen are strong functions of the energy. It would seem that a somewhat more accurate application of the method might result from using the averages expressed in Eqs. (9), (10), and (12).

Gray's discussion of stopping powers and average energies per ion pair is used to secure the values of these functions for the present investigation. Beyond that his formulation of the problem is not applicable to neutrons with

energies measured in tens of Mev. The wave-length of a 20 Mev neutron is $\frac{\lambda}{2\pi} = \lambda$ = 10.0 x 10^{-13} cm, of a 100 Mev neutron is about 0.5 x 10^{-13} cm, while the radius of the carbon nucleus computed from the scattering of 100 Mev neutrons [17] is 3.0 x 10^{-13} cm. As a result, elastic collisions do not occur in this energy region. The actual collision process, discussed in more detail below, may result in the production of protons, alpha-particles, residual nuclei, and neutrons, with energies between the primary neutron energy and a few Mev. Thus the energy transfer process is very different from that at lower energies, and calls for a somewhat different formulation.

Eq. (12) can be written in the form

$$\sum_i (\eta_i P_i) \chi_i - \left(\frac{N}{V}\right) \frac{1}{\Phi} = 0 \qquad (14)$$

where $X_i = \overline{\gamma_i k_i \sigma_i}$, and where it is supposed that the average of 1 / W S, as expressed by Eqs. (9) and (10), is nearly enough independent of energy over the primary energy spectrum to be removed from the integral indicated by the bar. In this equation the quantities in parentheses are to be considered as numerical constants which depend upon the nature of the ion chamber and the observed ionization, while the X_i's and Φ are to be considered as unknowns dependent only on the primary energy flux and the nature of the interaction between the neutron beam and the separate atoms, but independent of the special conditions of the experimental ion chambers. Thus, if we determine the ionization in a number of different chambers under suitable conditions, including identical neutron flux, then Eq. (14) will give a set of linear, simultaneous, homogeneous equation in the unknowns X_i and $1/\Phi$. If there is a sufficient number of equations, all of the unknowns but one can be determined.

The present investigation is limited to materials containing hydrogen, carbon, and oxygen. This method is applied, and values are determined for X_C, X_O, and Φ in terms of X_H. Numerical values are then secured by estimating X_H from data secured in an independent experiment.

Thus, even in the absence of detailed information about the collision process between the beam neutrons and the carbon and oxygen nuclei, we will be able to calculate both the energy flux of the beam and the energy transfer to hydrogenous solids. For the energy per cm^3 per second delivered to a solid at a depth greater than the maximum range of the recoil particles, is just

$$E_v = \Phi \sum_i n_i M_i X_i \tag{15}$$

Thus to the accuracy that the stopping powers and X_H can be computed, the energy dose to an arbitrary solid can be computed from the neutron flux

The function P_i of Eq. (14), defined in Eqs. (9) and (10), represents essentially an average reciprocal stopping power, since the average energy per ion pair, W, will be assumed constant. To be strictly accurate, the subscript i should be given values to differentiate the different types of collision with a single nucleus. It will be shown however that the reciprocal stopping powers are nearly constant enough to make this unnecessary. Apparently the stopping powers of the protons, alphas, and residual nuclei from a neutron-carbon collision can be characterized by a single number with sufficient accuracy for the present investigation.

Thus far all equations were expressed tacitly in cgs. units. For purposes of calculation, Eq. (14) is written in the form

$$\sum \left(\frac{f_i}{A_i} P_i\right) X_i - 10.43 \left(\frac{I}{V}\right) \left(\frac{1}{\Phi}\right) = 0 \tag{16}$$

where f_i is the fractional part by weight of element i in the wall material, A_i is the atomic weight of element i, P_i is the average of $(1/ S_i W_i)$ defined by Eqs. (9) and (10), S_i is the stopping power of the wall material relative to the gas in the cavity for the ionizing recoil particles, W_i is the average energy per ion pair expressed in ev/ion pair, $X_i = \overline{\gamma_i k_i \sigma_i}$ where γ_i is the energy of the average secondary particle expressed as a fraction of the energy of the primary neutron, k_i is the average number of ionizing recoils per collision σ_i is the cross section in barns for the production of one or more ionizing particles, the bar indicates an average over the primary energy spectrum weighted with the energy, I is the ion current in the cavity chamber in micro-micro-amperes, V is the volume of the cavity chamber in cc., and Φ is the primary energy flux in Mev/cm^2/sec. These are the units which are used in the calculations which follow.

If charge is measured instead of current, the equation becomes

$$(17) \qquad \sum_i \frac{f_i}{A_i} P_i X_i - 3.48 \times 10^3 \frac{Q}{t} \frac{1}{\Phi} = 0$$

where Q is the charge created in the chamber in esu/cc and t is the time of observation in seconds.

It is customary in this country at the present time to express energy dosages in units of the "roentgen equivalent physical", written rep. One rep=83 ergs per gram delivered energy, a number elevated to the position of a unit because it happens to be the rate at which energy is transferred to air when the ionization in air by a beam of X-rays is one esu/cc (one roentgen). Then Eq. (15) becomes in the units used in the present calculations

$$(18) \qquad E_v = 1.164 \times 10^{-8} \Phi \sum_i \frac{f_i}{A_i} X_i \qquad \text{rep/sec}$$

If Eq. (16) and (17) are solved for the primary flux and this is substituted in Eq. (18), the energy dosage is expressed in the equations

$$(19)\quad E_v = 1.214 \times 10^{-7} \frac{I_1}{V_1} \frac{\left(\sum_i \frac{f_i}{A_i} X_i\right)_2}{\left(\sum_i \frac{f_i}{A_i} F_i X_i\right)_1} \text{ rep/sec}$$

$$(20)\quad E_v = 4.05 \times 10^{-5} Q_1 \frac{\left(\sum_i \frac{f_i}{A_i} X_i\right)_2}{\left(\sum_i \frac{f_i}{A_i} F_i X_i\right)_1} \text{ rep}$$

where the subscript 1 indicates the cavity chamber with which the measurements are carried out, and the subscript 2 indicates the solid, presumably tissue, for which the energy dosage is calculated.

The density of the solid materials does not appear in any of the Eqs. (16) to (20). It is absent from Eqs. (18) to (20) because of the definition of the rep. It was dropped in writing Eqs. (16) and (17) because the product $n_i P_i$ is independent of density, as [redacted]. As a result, all stopping power functions will be calculated for materials of unit density, which will give the correct stopping powers for substitution in Eqs. (16) to (20).

Eq. (16) is the basis of the analysis of the ion chamber measurements made in the present investigation. Eqs. (19) and (20) are the basis of the application of the result to the calculation of energy dosages. It is noteworthy that, even though Eq. (16) is a homogeneous equation, so that the analysis will give X_C/X_H, and X_O/X_H, Eqs. (19) and (20) will allow calculation of the energy dosage without assigning a value to X_H. Thus the energy dosage problem is completely soluble in terms of quantities determined by the present ion chamber measurements, without recourse to data from other experiments, or detailed knowledge of the processes of energy transfer from the neutrons to the nuclei of interest.

The unique aspect of the present formulation lies just in the recognition that, even though our knowledge of the details of energy transfer is very vague, there is still a quantity, designated here by X_i, which characterizes ~~this~~ a collision and which can be determined by ionization measurements, and which is in fact just the quantity needed to make energy dosage calculations.

That this formulation has not been used before is not to be wondered at. At lower neutron energies the problem is quite different. Below about 10 Mev neutron collisions with the light nuclei will be elastic, and it will be sufficiently accurate for dosage calculation to assume isotropic scattering, as in Eq. (13). Since the energy transferred to the carbon and oxygen atoms in hydrogenous solids will be not over 10% of the total energy transfer, some anisotropy in the scattering of the neutrons by carbon and oxygen will not introduce a great error into the application of Eq. (15). Ion chamber measurements on neutrons of these energies are best made, not with a cavity chamber, but with a chamber sufficiently large so that the contribution to the ionization of the recoil nuclei from carbon and oxygen will be negligible compared to the ionization from the recoil protons from the hydrogen of the wall material. This is easily done, since the maximum range of the recoil nuclei from an 8 Mev neutron is 3.6 and 2.8 mm. for carbon and oxygen respectively, compared to 77 cms. for a recoil proton. The necessity for this arises from the almost complete lack of information about the stopping powers and average energy per ion pair for carbon and oxygen recoil nuclei. In his very detailed and careful discussion of the measurement of neutron flux by ionization methods, Gray [5] considers all these problems in detail, and then concludes that "the absolute determination of the neutron energy absorbed per unit volume of a solid hydrocarbon....is attended by an uncertainty of about 5%". Thus, in the neutron energy region of a few Mev, the present formulation is unnecessary.

ionisations will be strictly independent of energy.

Gray 5) has reviewed the experimental evidence in detail. He concludes that 36.0 e.v. is the best estimate of the value of W for a proton of initial energy 2.5 Mev or higher, while W is about 10% higher for a proton of initial energy 0.25 Mev. He gives values of W for alpha particles as 4% lower than for a proton of the same velocity. He also lists value of W for particles of given instantaneous energy to be about 4% less than for particles of a given initial energy. (These experimental values include the effect of delta rays).

Use of Eqs. (9) to (12) would require values of W for the spectrum of instantaneous energies of all the secondary particles. The approximate constantcy of W allows the use of Eq. (14) and subsequent equations, instead. Due to the inadequacy of the data on W at very high and very low energies, and due also to uncertainty over the exact nature of the ionizing secondaries arising from the neutron beam studied here, it is not possible to say precisely what is the best average value of W to use. We shall adopt here the value

$$W = 36.0 \text{ ev / ion pair}$$

with the understanding that it carries an uncertainty of about 5%

8. - Average energy per ion pair

It is well known that the average energy spent by an ionizing particle in producing an ion pair is on the order of 35 ev/ion pair, and is more or less independent of the energy, mass, and charge of the ionizing particle, and of the nature of the gas in which the ionization is produced. These properties are reasonably well accounted for by the latest theories[21] though the agreement between theory and experiment is not sufficiently good to allow use of other than experimentally-determined values in calculations involving ionization yields, such as the present.

The value of W, the average energy per ion pair, with which we are here concerned is not just that for a fast proton or alpha particle. Lea estimates[18] that for protons between 1 and 10 Mev, about half the total ionization is primary, and about half is due to the delta rays (electrons of sufficient energy to produce secondary ionization). He further estimates that only about 1% of the delta rays are of energy greater than 1000 ev. (These calculations were made for tissue, but apply qualitatively to air , or to the material used in the present investigation). Thus in the present case about half the ionization will be produced by heavy particles with energies of tens of Mev, and about half by electrons with energies of hundreds of ev. The appropriate value of W, then, arises from a combination of these two quite different cases. Theory[14] shows that we can expect that the W for the primary ionisations by heavy particles with energies above 1 Mev will remain essentially constant, while the W for the ionisations by electrons with energies in the neighborhood of 1000 ev will be in fact somewhat dependent upon electron energy. Since the energy distribution of the delta rays will be to some extent dependent upon the energy of the primary heavy particle, we cannot expect that the actual value of W for all the

2. - Average Energy per ion pair

All of the determinations of the average energy per ion pair have been summarized and discussed critically by Gray [5]. From this work we shall use the value 35.5 ev. / ion pair. While this was determined for protons and alpha-particles in the energy range of a few MEV, there is good reason to believe that this quantity remains essentially constant at higher energies [14]. This value of W will be used for all of the ionizing secondaries produced by neutrons.

3. - Proton stopping powers

The experimental and theoretical data available on the stopping power of protons relative to air has been discussed and summarized by Gray [5]. He has tabulated the relative atomic stopping power for protons of hydrogen, carbon, and oxygen, up to 14 Mev. Using the Bethe formula [13], his values have been extrapolated to 200 Mev. There is good reason to believe that this is a reliable procedure, since the experimental and theoretical difficulties lie in the region below one Mev.

The Bethe formula was fitted to Gray's values at 14 MEV by taking for the ionization potential of air 80.5 ev., [13] and solving for the ionization potential of hydrogen, carbon, and oxygen. These turned out to be 11.1, 67, and 96 ev, respectively. Then, using these values, the relative stopping powers were calculated from 4 Mev to 200 Mev. The results, along with Gray's values, are given in Table 1. As is to be expected, the values calculated by the simple formula used here, diverge appreciably from the values given by Gray for energies below about 8 Mev, since no K-shell correction has been used. A simple calculation showed that the Fermi effect need not be included in proton stopping powers for energies below about 1.5 Bev.

Table 1.

Relative atomic stopping powers for protons. Columns headed "Gray" are taken from Reference 5, p. 77. Columns headed "calc." are calculated by the Bethe formula, adjusted to Gray's values at 14 ~~MEV~~ Mev.

PROTON ENERGY ~~MEV~~ Mev	HYDROGEN		CARBON		OXYGEN	
	Gray	Calc	Gray	Calc	Gray	Calc
.05	.380		-		-	
.1	.358		-		-	
.2	.316		-		-	
.4	.269		.926		1.031	
.6	.248		.918		1.045	
.8	.238		.909		1.051	
1.0	.231		.903		1.054	
1.5	.221		.894		1.060	
2.0	.214		.889		1.063	
2.5	.209		.885		1.066	
3.0	.206		.883		1.068	
3.5	.203		.880		1.069	
4.0	.201	.197	.878	.863	1.070	1.069
6.0	.194	.193	.872	.862	1.072	1.072
8.0	.190	.190	.867	.859	1.074	1.075
10	.188	.188	.863	.860	1.075	1.075
12	.186	.186	.860	.858	1.076	1.076
14	.185	.185	.857	.857	1.077	1.077
20		.182		.855		1.080
25		.181		.854		1.081
50		.177		.852		1.083
100		.174		.850		1.086
150		.172		.849		1.087
200		.171		.850		1.087

In using these relative atomic stopping powers to compute relative stopping powers for various materials, the delta rays will be ignored. The justification for this lies simply in the very short ranges of low energy electrons. A 1000 ev electron has a range in air of probably considerably less than 50 microns. Thus the delta rays originating in the wall material of ~~the~~ conventional ion chambers will not contribute appreciably to ionization measured in the gas of the chamber.

4. - Constants of the Materials Used.

The materials used in these ionization studies were chosen so as to give a wide range of composition of the three atoms carbon, hydrogen, and oxygen. The composition and density of the materials used are listed in Table 2. The columns headed "f_i/A_i" give the parts by weight over the atomic weight for carbon, hydrogen, and oxygen. These are convenient coefficients to use in the calculations involving total ionization. The source of the information listed in table 2 is given in the following paragraphs.

Carbon: The carbon used was a good quality, fine-grained material. The density of the samples used varied slightly, with an average about that tabulated. These density variations, within about $\pm$ 2%, were disregarded except in cross section measurements, where the measured density of the sample was used in the calculation.

(by a professional, organic analyst)

Paraffin: The composition was determined by direct analysis, and the density was measured. This was exceptionally pure and uniform.

Polystyrene: No analysis was made, beyond measurement of the density, which was found to be uniform between different samples. It was assumed that the polystyrene was pure, polymerized styrene.

Lucite: This is the trade name of the methyl methacrylate resin produced by the duPont Co. The composition was determined by direct analysis of one sample, and the density by measurement of several samples. The density was uniform.

Plexiglass: This is the trade name of the methyl methacrylate resin produced by Rohm and Haas Co. The composition was determined by direct analysis, and the density by measurement. The density was uniform.

Water: That used was tap water. Composition and density assumed to be the values for pure water.

Oxalic Acid: That used was in the crystalline form, reagent grade, the

water of crystallization taken as stated by the manufacturer. No density measurement was made.

Lactose: Same comments as oxalic acid.

Table 2

Composition and density of materials used as ionization chamber walls.

Substance	Formula	Density	Pts By Wt.-f_i C	H	O	f_i/A_i C	H	O
Carbon	C	1.59	1.00		-	.0833	-	-
Paraffin	$CH_{2.07}$	.909	.852	.1478	-	.0709	.1466	-
Polystyrene	C_8H_8	1.05	.922	.0775	-	.0768	.0768	-
Lucite	-	1.18	.608	.0802	.312	.0506	.0796	.0195
Plexiglass	-	1.18	.601	.0780	.321	.0501	.0774	.0201
Water	H_2O	1.00	-	.112	.888	-	.1110	.0555
Oxalic Acid	$(CO_2H)_2 \cdot 2H_2O$	-	[illegible]	[illegible]	[illegible]	[illegible]	[illegible]	[illegible]
Lactose	$C_{12}H_{22}O_{11} \cdot H_2O$	-	.400	.0672	.533	.0333	.0666	.0333

11 .191 .0480 .762 .0159 .0476

Using the atomic stopping powers of Table 1 and the composition coefficients of Table 2, stopping powers have been computed for the substances used as ion chamber wall material. These are listed in Table 3. The table gives the reciprocal of the stopping power at various energies, and the average of these stopping powers from 0 up to the energies tabulated. The calculations were made with the formulas

$$S = \frac{A_a}{d_a} \sum_i \frac{f_i}{A_i} s_i \quad , \quad i = C, H, O$$

$$\overline{1/S} = \frac{1}{E} \int_0^E \frac{1}{S} \, dE$$

where s_i is the relative atomic stopping power from Table 1.

A_a is the average atomic weight of air = 14.55, and d_a is the density of

air = 1.205×10^{-3} at 20° C. and 76 cms.

The values of the stopping powers below 1 Mev are not at all certain. Thus the averages $\overline{1/S}$ can hardly be expected to be accurate to more than several percent. The difference between the values of 1/S and $\overline{1/S}$ at a given energy may be taken as an indication of the amount of uncertainty in the stopping powers to be used in the calculations.

In calculating Table 3, Gray's values of the atomic stopping powers were used up to 14 Mev and the extrapolated values beyond that. These stopping powers were plotted, and values read from the graphs to secure sufficiently small intervals to make the numerical integrations. The density of the substances listed in Table 3 was taken as unity for the stopping power calculations, since this is the appropriate stopping power for use in Eqs. (16) to (20).

Table 3

Reciprocal stopping power for protons relative to air for substances used in ionization chamber walls. Rows marked "1/S" give the reciprocal of the relative stopping power for protons at the energy listed, for the substance listed. Rows marked "$\overline{1/S}$" give the average of 1/S from 0 out to the energy listed. Density taken as unity.

Energy		0.0	.4	1.0	3.0	10	30	100	Mev
Carbon	1/S	0.99	1.07	1.10	1.12	1.15	1.16	1.17	$X10^{-3}$
	$\overline{1/S}$	0.99	1.03	1.06	1.10	1.13	1.15	1.16	$X10^{-3}$
Paraffin	1/S	0.38	.79	.84	.89	.93	.95	.96	$X10^{-3}$
	$\overline{1/S}$	0.38	.58	.72	.82	.89	.92	.95	$X10^{-3}$
Polystyrene	1/S	0.54	.90	.95	.99	1.02	1.04	1.05	$X10^{-3}$
	$\overline{1/S}$	0.54	.72	.84	.93	.98	1.02	1.04	$X10^{-3}$
Lucite	1/S	0.57	.95	.99	1.02	1.05	1.06	1.07	$X10^{-3}$
	$\overline{1/S}$	0.57	.76	.89	.97	1.02	1.04	1.06	$X10^{-3}$
Water	1/S	0.50	.95	.98	1.01	1.03	1.03	1.04	$X10^{-3}$
	$\overline{1/S}$	0.50	.71	.86	.95	1.00	1.02	1.03	$X10^{-3}$
Lactose	1/S	0.62	1.00	1.03	1.05	1.08	1.08	1.09	$X10^{-3}$
Oxalic Acid	1/S	~~0.70~~ 0.74	~~1.06~~ 1.08	~~1.08~~ 1.10	~~1.10~~ 1.11	~~1.11~~ 1.12	~~1.12~~ 1.12	~~1.12~~ 1.13	$X10^{-3}$

Proton ranges of sufficient accuracy for the present experimental data have been calculated by approximate methods from accurate range data in certain materials. The range-energy relation for carbon is given over a wide energy region in Reference 15. A range-energy relation for paraffin up to 15 Mev is given in Reference 16, which also gives accurate stopping numbers for hydrogen and carbon up to 15 Mev, and for oxygen up to 3 Mev. Reference 15 gives stopping cross sections up to 10 Mev. In Figs. 1 and 2 are given the range-energy curves for carbon, paraffin, and polystyrene. Carbon is taken from ref. 15. Paraffin is from ref. 16 up to 15 Mev, and is computed from the carbon curve for higher energies. Polystyrene is interpolated between the carbon and paraffin curves up to 15 Mev, and is computed from the carbon curve at higher energies.

Certain other substances may be of interest, and factors for computing their ranges from the carbon range are given in Table 4. "Meth. Resin" refers to either of the methylmethacrylate resins, Plexiglass or Lucite, taken to have the composition $C\ H_{1.56}\ O_{.394}$. Tissue is taken to have the composition $C\ H_{8.6}\ O_{4.0}$, which is arrived at by taking the formula for wet tissue given by Lea, [12] taking the 4% nitrogen by weight and splitting it between carbon and oxygen.

Table 4

Proton ranges in various materials relative to the range in carbon, all ranges in mg./cm.^{2}

Energy, Mev	1	3	10	30	100
Meth. Resin	.94	.93	.92	.92	.92
Water	.65	.60	.55	.55	.56
Tissue	.98	.95	.93	.92	.93

The computation of the approximate ranges is made in the following fashion: The well-known Bethe theory of energy loss by charged particles[13] gives the range R of a charged particle in the form

$$R = \text{constant} \times \int_0^E \frac{E\,dE}{\sum_i \frac{f_i}{A_i} B_i} \quad mg/cm^2$$

where B_i is the atomic stopping number, defined in the conventional fashion, for atom of type i, and the other symbols are those used earlier in this paragraph. From this we may write

$$\frac{R_2}{R_1} = \frac{\left(\sum_i \frac{f_i}{A_i} B_i\right)_1}{\left(\sum_i \frac{f_i}{A_i} B_i\right)_2}$$

where the subscripts 1 and 2 indicate two different substances, and the ranges are both in $mg./cm.^2$. This is valid provided that the ratio on the right hand side is approximately independent of energy. This is in fact the case for the substances for which approximate ranges have been given in terms of the range in carbon. Figures 1 and 2, and table 4, have been computed by estimating the average value of this ratio for the energies given.

This method of range calculation, as well as the stopping power calculations, are based upon the assumed validity of simply adding stopping numbers (or relative stopping powers). While it cannot be exactly correct to disregard the effect of chemical bonds, it has been shown experimentally that it is valid to do so within the range of accuracy of ordinary experimentation.[5]

IV - Experimental Results

1. Preliminary Measurements. The Extrapolation Chamber

When it was first decided to investigate the energy transfer problem with the 100 Mev neutron beam, there was very little information available about the secondary particles to be expected. Cloud chamber pictures at that time had already shown that in at least some of the neutron collisions with carbon and oxygen nuclei, stars were formed, some of the prongs of which were relatively short range, heavily-ionizing particles. Thus it was considered possible that most of the energy delivered to a solid by the neutrons was dissipated by particles of very short range in air, perhaps as small as a few millimeters. In order to investigate this, a variable-spacing parallel plate ionization chamber, called here an "extrapolation chamber", was designed.

The extrapolation principle, the origin of which was discussed above, has been very extensively used in X-ray and gamma-ray investigations. As it is generally used, the ionization between the plates of a parallel-plate chamber is observed as a function of the spacing of the plates. If the measured ionization is proportional to the plate spacing, then the chamber is a true cavity chamber as defined in the present discussion, and the Bragg-Gray equation may properly be applied. For low energy radiation the spacing may have to be very small before this condition is met. The name is derived from the notion that, if the volume ionization is plotted against the spacing, it may be extrapolated to zero spacing, thus giving the volume ionization for an infinitely thin chamber.

The extrapolation chamber as designed for the present purpose is shown schematically in Figure 3. When the plate spacing is very small, it is a plastic sphere, 5 inches in diameter. Part A is a screw, 2 inches in diameter, with a pitch of 10 threads per inch. The surface between parts B and C is a plane through the center of the sphere. Part C is fastened firmly to part B by

eight screws, one of which is shown. Part D fits snugly into part C to complete the sphere, but slips off in order to mount the chamber on the electrometer. The top, round surface of screw A is divided so that the screw can be set to the nearest thousandth of an inch. Surfaces are rendered conducting by painting with a coating of graphite. By putting similar graphite coatings on weighed pieces of mica, it was found that the graphite coatings used were not thicker than 0.1 mg./cm^2. [a] The anode is the bottom surface of screw A, and the cathode and collecting electrode is the upper surface of C. The collecting electrode is separated from the guard ring by a very fine line scribed on the upper surface of C. This isolates a central, circular electrode 1 3/4 inches in diameter from the guard ring by line not over a few thousandths of an inch wide. [b] Connection to the anode, and to the cathode guard ring is made by graphite paths that lead through small holes to small screws on the surface of the sphere. Electrical contact with the collection electrode is made through a small hole (#80 drill, 0.0135"diameter) which goes through part C about 1/16" off center, and which meets on the lower side of C a counterbore 1/8" in diameter and 0.010" deep, the hole and counter-bore being coated with graphite. In Figure 3 the collecting electrode and guard ring are shown as very heavy lines for clarity, though in the chamber the graphite coatings are of negligible thickness.

The extrapolation chamber was made from Lucite. It was made spherical because at the time it was designed, the neutron beam of the 184" Cyclotron was not well collimated, and it was believed there was a strong isotropic background radiation. In order to measure this background, it was felt that

[a] The most convenient form of graphite used was colloidal graphite suspended in ethyl alcohol, furnished by Acheson Colloids Corp., with the designation "Dag" Dispersion No.154.

[b] This method is due to G. Failla.

an essentially non-directional detector would be needed. By the time the experimental work had progressed to serious ionization measurements on the neutron beam, the problems of shielding and collimation had been solved, and it was possible to work in a sharply-defined beam. As a result, the sphericity of the extrapolation chamber played no role in the experimentation.

The Lindemann electrometer used with the extrapolation chamber was essentially that described in reference 18. The electrometer circuit was a conventional null-type circuit, in which the accumulated charge is calculated from the voltage required to return the electrometer needle to zero by pulling the charge onto a capacity of known value here (10.22 cms.). Because the ion chamber was placed in an external radiation field, a bridge-type circuit, as described in Ref.18, was not used, since the balancing condenser would be irradiated at the same time as the detection chamber.

The method of using the extrapolation chamber is as follows: A battery is attached between the anode connection and the guard ring connection, with sufficient voltage to give about 100 V/cm. field. With D removed, the chamber is placed on the electrometer, bringing the flexible contact needle of the Lindemann electrometer assembly into contact at the center of the bottom side of C, as indicated by the arrow. The needle at this time is grounded to the case of the electrometer assembly, which is also connected to the battery negative and to the guard ring. Then the chamber is carefully removed from the electrometer, part D slipped into place, and the chamber placed in the desired position and irradiated. Then part D is removed, the chamber placed back on the electrometer, and the needle ungrounded just before making contact with the collection electrode. Just at the instant of contact, the compensating voltage is applied, so as to prevent the Lindemann fiber's sweeping far off scale and producing a false reading due to hysteresis in the fiber system.

The battery is left connected to the chamber during the entire process, and the battery negative is kept grounded to the electrometer case through a wire sufficiently long to allow moving the chamber to the place of irradiation. Thus the only make and break is at the collection electrode, and this is done in a field-free region, excepting for contact potentials and a small field due to the acquired charge. Whenever the a-c fields were large enough to produce appreciable readings due to a-c pickup, the entire chamber and its battery system were shielded during the make and break process.

The sensitivity limitation was the background charge, as determined by a blank run. This was never the background radiation, but was a "false" background due apparently to induced voltages, contact potentials, etc. The order of magnitude of the background observed was about 1% of the charge given by 1 mg. of Ra. at a distance of 30 cms, for the maximum usable chamber spacing. The background was essentially constant with spacing of the chamber, but depended upon the care with which the manipulations were carried out. Under the sometimes far from ideal condition which obtained in work in and near the cyclotron beam, the background was larger than for the best laboratory conditions. The heavy exposures available in the beam, however, made the background corrections sufficiently small so that the accuracy remained about a few percent, for a single reading.

The screw zero was determined by measuring the capacity of the chamber against the fixed condenser. The usable spacing was determined by plotting Cd against d, where C is the measured capacity of the chamber and d is the spacing between the electrodes. Cd was found to be constant, as it must be for a proper parallel-plate condenser, from a spacing of .025 mm. up to 1 cm., within 1/2%. Beyond 1 cm. Cd was no longer constant, indicating that the guard rings were not maintaining a parallel field over the collection electrode. All

subsequent measurements were made with spacings not over 1 cm.

The extrapolation chamber was tested, and the techniques of handling it were developed with Ra and Ra-Be sources. Very great care was needed in manipulating the chamber, and much time was consumed in developing the rather special techniques needed to keep the background of induced charge low. When it was possible to make reliable measurements on the fixed sources, the observed volume ionization was independent of electrode spacing within the error of measurement from about .01 cm. to 1.0 cm. Then a series of measurements was made with the extrapolation chamber in the neutron beam. The method was to put the extrapolation chamber, and a suitable monitor, in the neutron beam simultaneously. A series of measurements was made of the volume ionization in the extrapolation chamber relative to the monitor, as a function of the electrode spacing. The results of the best series of observations were as follows:

d in cm.	.012	.020	.030	.055	.081	.131	.207	.385	1.01
monitor #1	2.48	2.58	2.45		3.13?				
monitor #2				2.59		2.61	2.66	2.51	2.49

The first row gives the electrode spacing in cms. The next two rows give the ratio of the charge per unit volume observed in the extrapolation chamber to that observed in the monitors. Monitor #1 was a Victoreen chamber with a full scale sensitivity of 250 mr. Monitor #2 was a Lauritsen electroscope with a full scale sensitivity of 6 mr. The question mark indicates a reading on the monitor very unreliable because of its small value. There is no indication of increased volume ionization in the extrapolation chamber for the entire span of the measurements, indicating that a chamber with dimensions less than a centimeter satisfy

the cavity conditions.

Although it has no direct connection with the central problems of the present investigation, it is interesting to note that the spherical chamber was found to be very nearly isotropic in sensitivity. The maximum sensitivity was for radiation entering through the side of the chamber, this giving about 5% greater charge than for radiation entering through the bottom. This is presumably due to the fact that in the latter case the column of ionization from each secondary is nearly parallel to the electric field, while in the former case it is more nearly perpendicular to the field. This produces less recombination for radiation entering from the side, and hence somewhat greater observed charge. This is a well-known phenomenon, having been discussed in detail many years ago by Jaffe in his work on the theory of recombination[8]. Since no attempt was made to interpret closely in any absolute sense the measured ionization in the extrapolation chamber, no correction was made for recombination. The field was kept at about 100 V./cm., which was found to be within a few percent of saturation voltage by measuring charge for a given radiation exposure as a function of voltage. The field was kept at about this value for the series of measurements tabulated above.

An attempt was made to investigate further the ionization as a function of size of chamber by using various types of the commercial chambers available. These were unsuccessful due primarily to the fact that the beam collimation made use of a chamber more than a few inches in size impractical outside the shielding, and that very high background of scattered radiation inside the shielding gave the measurements a very different significance from those taken outside. As a result, these attempts led to little additional information beyond confirmation of the existence of a high background inside the shielding.

2. The Shallow Ionization Chamber. Transition Curves.

When the extrapolation chamber measurements had made it clear that there was no difficulty in constructing a chamber which meets the cavity conditions, at least with regard to range of particles crossing the chamber, it was decided that the next step was to investigate the observed ionization as a function of thickness of secondary-producing material, to find the depth of material required to give maximum ionization. To achieve this an ionization chamber was constructed with a 1/2" slab of polystyrene for one side, .001" polystyrene for the other side, the periphery of the chamber being a 1 1/2" diameter hole in a piece of 1/16" micarta. The surfaces of the polystyrene were rendered conducting with graphite, and the current was read on an electrometer circuit. The first measurements made with this chamber in the neutron beam were a study of the "backscatter", that is to say, the current in the ion chamber due to material on the downstream side (with respect to the direction of neutron flow) of the chamber. It was found that the backscatter current was about 5% of the total current, and was identical within the accuracy of measurement, at that time a few percent, for carbon, polystyrene, paraffin, and Lucite. While the full significance of this equality of the backscatter current was not realized until much later in the experiment, it was at once clear that this fact made it possible to compare total ionization due to different H-C-O materials with an ion chamber the back and sides of which were made from any suitable material containing only H, C, and O.

A schematic cross section of the final form of the chamber developed to make these measurements is shown in Figure 4. The body of the chamber is a 6" x 6" x 1/4" piece of plastic (Lucite, Plexiglas, or

polystyrene). On one surface a circular cavity is cut, 1 1/2" in diameter and about 1/16" deep (1.5mm.). The bottom surface of this cavity is coated with graphite and a 1" circle is scribed in the graphite, creating a collection electrode and a guard ring, by the technique described in the discussion of the extrapolation chamber. Across the open surface of the circular cavity is a foil made by sputtering Be on Formvar. The Be coating is sufficiently conducting to form the anode of the chamber. The foil adheres to the surface of the plastic without the use of any adhesives other than a small amount of water or alcohol used to pull it into place. [c] The thickness of the foil is estimated to be not over 0.1 mg./cm^2.

Electrical contact with the foil is made by a trail of graphite which leads along the surface of the plastic to a hole which connects in turn to a tapped hole to which the external lead is connected. The electrical connection to the guard ring is made through a graphite-coated hole leading through the center of the plastic to a similar tapped hole, not shown. Electrical contact to the collecting electrode is made through the system of holes shown. As with the extrapolation chamber, the hole leading into the electrode is as small as can conveniently be drilled, that is, a #80 drill. The back side of the plastic is either covered by a grounded carbon piece as shown, or is coated with a heavy graphite coating, to provide electrical shielding. A 1/32" Micarta spacer is used on the front side to protect the foil from the slabs of secondary-producing material

---

[c] This foil was prepared and mounted by Dr. Hugh Bradner of this laboratory.

The several parts of the chamber are all 6" x 6" squares, screwed together at the corners by screws not shown in the diagram. The unit is mounted on top of a portable electrometer unit, the "Zeus meter". The Zeus circuit, developed at the Metallurgical Laboratory of the Manhatten Project during the war, is a bridge circuit using two VX32 tubes, with a sensitivity of 2$\mu\mu$ amps. full scale. In normal use, the grid of one tube is connected to a probe which runs into the center of the ionization chamber built into the body of the unit. The walls of this chamber are normally insulated from the case and connected to a high positive voltage. The modification for use in the present investigation consisted only in grounding the walls of the built-in ionization chamber, and running the probe straight up through the top of the unit so that it projected about one inch. This is marked "electrometer input" in Figure 4. A close-fitting plastic jacket was placed around the 1/8" brass rod used as the probe, where it runs through the built-in ion chamber. This rod fitted a hole in the plastic body of the shallow chamber, furnishing electrical contact with the collecting electrode.

The chamber, when firmly mounted on top of the Zeus cabinet, formed a convenient, portable unit. The Zeus cabinet is 12" high and 8" square, so that the unit could be mounted directly on the experimental neutron bench, shown in Figure 5, putting the ionization chamber in the center of the beam. The collimating system, indicated diagrammatically in Figure 5, produces a neutron beam diameter of approximately 3" along the neutron bench. This "diameter", determined by exposing film to the beam, has been confirmed by measurements made with carbon detectors using the 20 Mev threshold reaction, $C^{12}(n, 2n)\ C^{11}$. The carbon detectors showed a flat-topped profile, with an intensity just inside the

edge of 2000-4000 times the intensity just outside. This sharp gradient made it possible to have the circuits just a few inches outside the beam, and still collect negligible ionization in the free volume of the circuit cabinet.

Two such units were constructed, so that one could be used as a monitor. The normal method of observation was to line the two shallow chambers up in the neutron beam, with the monitor on the upstream side (with reference to the direction of neutron flow). They were lined up by optical means with the predetermined center of the beam, with an accuracy of about 1/8". It would have been possible to line them up with very much greater accuracy, but there seemed to be no reason for doing so. The monitor would be assembled with sufficient material on both sides so that only the neutrons could reach the chamber from outside. With the monitor on the upstream side of the detector chamber, the changes made in the detector chamber would have no effect on the monitor, so that the ratio of detector current to monitor current was a valid estimate of the relative effect of the parameter under study, free from beam intensity fluctuations. Under certain circumstances it was desirable to put the monitor on the downstream side of the detector. When this was done, the material in the beam path to the monitor was kept constant, by simply transferring material from one side of the detector chamber to the other. The distance from the monitor to the detector was in these cases at least 6 feet, so that the beam attenuation as seen by the monitor was constant.

Using these methods, transition curves were studied for a number of substances. Figure 6 shows a typical set of transition curves, for four different substances. The scales of abscissae are displaced so

that the initial points will not overlap. The points plotted are the ratios of observed currents, detector relative to monitor, normalized to unity at zero thickness of added material. This minimum ionization represents of course secondaries arising in the air, in the thin foil on the front side of the chamber, and in the material in the back of the chamber. These measurements were made with the monitor downstream from the detector, because this arrangement gave the minimum current for zero added material due to the absence of secondaries from the monitor assembly.

The same set of experimental points is replotted in Figure 7, after a correction has been made for neutron absorption by a method described below. The scale of abscissae in Figure 7 is now the energy in MEV of a proton having a range equal to the thickness of material. These energies are taken from the range-energy curves of Figures 1 and 2, except for copper, which is from Reference 15. It seems likely that the coincidence of the three curves paraffin, polystyrene, and carbon along a straight line is real for the same result was observed under various circumstances of taking transition curves. An important feature of these curves is the energy at which each curve levels off, and the values are seen to be fairly consistent and reasonable.

Transition curves were investigated for very thin layers of polystyrene, with the results shown in Figure 8. Curve A was taken first, the two runs indicated as #1 and #2 being separated in time by about 12 hours, without disturbing the apparatus. The several breaks in the curve seemed to be quite interesting, and the experiment was repeated, giving curves B and C. Curves A and C should be comparable, since for both the

chamber was in about the middle of the neutron bench with no solid matter in the beam between the chamber and the wall of the cyclotron. Curve B was taken simultaneously with curve C, and was made in the same way except that a piece of copper, 0.56 mm. thick (16 MEV proton range), was placed immediately upstream for the purpose of cutting out short-range secondaries originating in the air. The same points are replotted in figures 9 and 10, using proton energy as the scale of abscissae. This time there is no correction for neutron absorption, since this effect is negligible at these thicknesses. In addition, figure 9 contains a few points obtained for carbon and paraffin at these thicknesses, taken at the same time as the points designated run #2 in curve A. The existence of some fine structure is hardly to be doubted, but the discrepancies between curves A and C indicate the presence of unknown factors, which makes the interpretation of the observed fine structure uncertain.

Figure 8 shows a reverse transition curve for polystyrene. This was taken with the monitor upstream from the detector, and with the detector chamber turned around so that the thin foil was on the downstream side. The current relative to the monitor was then observed as thin sheets of polystyrene were brought up to the chamber on the rear side. The flat plateau is certainly real, since points were obtained out to 3 cms., all lying on the plateau shown within 2%. Since the cloud chamber photographs and the film studies of the neutron and deuteron beams as well as predictions based upon momentum and scattering considerations, have made it entirely clear that only a negligible fraction of the secondaries originating upstream could cross the chamber and then be scattered back through an angle in the neighborhood of 180°, it is quite safe to assume

that the increase in ionization indicated in Figure 11 is due to secondaries created on the downstream side of the chamber. Then, taking the value of the plateau from Figure 8, and using Figures 6 and 7 to correct for the fact that the reverse transition curve was taken with only 0.48 mms. of polystyrene upstream, it can be computed that the downstream secondaries contribute 5.3% of the maximum ionization current, and 4.9% of the ionization current computed for no neutron absorption, with polystyrene.

This result was checked directly by measuring the current from the downstream secondaries as a function of thickness of material upstream, and it was in fact constant, and of the value just stated. It was the same for carbon, paraffin, polystyrene, and Lucite, and increased by a factor of approximately two for Cu and Pb. Only a few measurements were made on these last two elements, so that the numerical results are not felt to be reliable enough to quote.

An attempt was made to improve the transition curves by getting a more nearly proton-free beam, by using an evacuated tube upstream of the ion chamber. This was a brass tube, 6 feet long, closed on its upstream end with 0.05 mm. brass, and on its downstream end facing the ion chamber, with 10 mg./cm^2 mica. The tube was presumably large enough in diameter to clear the beam, the smallest clearance being a 3 1/2" flange supporting the mica, at the place where the beam was about 2 3/4" in diameter. While the general behavior indicated that the tube was properly aligned so that it was not scattering secondaries into the chamber, absolutely no change was produced by evacuating the tube to 50 microns. It was expected that the removal of the air would decrease the observed ionization

when the chamber was fronted only with the thin foil. From the absence of any effect, it is inferred that the secondary particles from the distant brass end of the tube and from the near mica window effectively contribute the same ionization as the six feet of air removed.

3. Bad Geometry Neutron Attenuation

The decrease in observed ionization with increased thickness of material, in the transition curves of Figure 6, can only be due to attenuation of the neutron beam. It was found possible to determine this attenuation as follows: Some measurements were made to determine how much copper was needed to stop all the secondaries from paraffin. It was found that there was a small but appreciable number of protons from paraffin getting through 1.3 cms of copper (100 Mev proton range), but none at all could be detected through 2.54 cms. of copper. So a series of bad geometry attenuation curves were taken where 2.54 cms. of copper was between the material being tested and the chamber, the material being otherwise as close as possible to the chamber. The monitor was upstream of the detector for these measurements.

It was found that the attenuation measured under these circumstances was accurately exponential out to about 10 cms. from the front of the ion chamber. At that distance, the attenuation became more rapid, indicating presumably the transition from bad geometry to good geometry attenuation. [d]

---

[d] "Bad geometry", as the term is used here, is essentially equivalent to an infinite scatterer in an infinite beam. "Good geometry" means that no scattered particles reach the detector. The former term will be restricted to attenuation within 10 cm. of the detector, the latter to attenuation at distances greater than 2 meters. This distance was found experimentally to be sufficient to give attenuation measurements independent of distance.

In this region the observed attenuation curves matched very accurately the transition curves for the corresponding material. From the $T_{1/2}$ values measured in this fashion, it is possible to compute bad geometry cross sections. These results are tabulated in Table 5.

Table 5 - Bad Geometry Half-intensity Thicknesses and Cross Sections for Various Substances.

Material	Carbon	Poly-styrene	Paraffin	Water	Plexi-glas	Copper
$T_{1/2}$, cms.	41.7	51.5	57.5	55.9	47.0	12.0
σ_{abs}, barns	σ_c = .21	σ_H = .059		σ_O = .27		σ_{Cu} = .69

The values for $T_{1/2}$ given in Table 5 were simply read from a logarithmic graph of the experimental points, and no error has been computed. The value of σ_H tabulated is the mean of the values computed separately from the polystyrene and paraffin observations, using the computed σ_C. These were .069 and .049, respectively. Similarly, the tabulated value of σ_O is the mean of the two values computed from the water and Plexiglas observations, namely .254 and .283, respectively. This makes it clear that the accuracy of the observations is not high. It would be reasonable to attach to all the tabulated cross sections a mean error of $\pm$ .02 barns. The densities and compositions of the materials are those listed in Table 2.

The attenuation correction used to get Figure 7 from Figure 6 was taken from the bad geometry attenuation curves on which Table 5 is based. To make this correction rigorously would be difficult, considerable since the secondaries reaching the ion chamber come from a depth of

material, about 7 cms. for paraffin. Fortunately, the attenuation is sufficiently small so that this is not a large effect, and no great error would be introduced by disregarding it entirely. It has been taken into account in a rather crude fashion, as follows: using the curves of Figure 6, an "ionization centroid" has been computed using the formula

$$\bar{x} = \frac{1}{I_m} \int_0^{I_m} x\,dI$$

where $\bar{x}$ is the computed centroid in cms., I_m is the maximum value of the observed ionization current, and x is the depth of material producing the ionization as a function of the measured ionization current I. The results of the very approximate numerical integration are given in Table 6, in which x_m is the depth of material producing maximum ionization current.

Table 6 - Ionization centroids for various materials.

Material	carbon	polystyrene	paraffin	copper
$\bar{x}$ in cms.	.50	1.1	1.1	.12
$\bar{x}$ in proton MEV.	27	34	33	26
$\bar{x} / x_m$	.15	.18	.18	.10

The method of using these centroids was then to use, as the effective thickness of material for purposes of estimating the attenuation, one-half the actual thickness up to a thickness of twice the centroid, and beyond that use a thickness measured from the centroid. Beyond the depth of material from which secondaries reach the chamber, the attenuation correction could be taken from the observed transition curve itself, without any necessity for considering effective thickness. This in fact would in theory be preferable to using a correction determined from a curve in which the secondaries originated in a different material.

It however is objectionable in the sense that each curve would automatically correct itself to a constant value, independent of any errors in observation. It seemed preferable to use a completely independent set of observations to get the correction, so that the flatness of the plateaus in Figure 7 can be taken as an indication of the accuracy of measurements. These remarks do not of course apply to the copper curve, in which case it was necessary to use the observed curve to correct itself.

In the paraffin and carbon curves of Figure 7, it is seen that there is a slight tendency for the points to be high in the middle of the plateau and drop low toward the end. This has been observed in a number of other transition curves corrected in the same fashion. While the effect always lies within the errors of observation, its occurrence in about half the transition curves makes it seem like a real tendency to over-correct for attenuation by the technique described. If the effect is real, it is not over a percent or two, so no great error can be introduced by it.

The calculations from which the figures of Table 6 are taken were only approximate, since the crudeness of the concepts does not justify an accurate computation. Thus no significance can be attached to the difference in $\bar{X}$ expressed in proton MEV for polystyrene and paraffin, but the difference between carbon and paraffin is perhaps significant.

4. Good Geometry Neutron Attenuation

Interpretation of the ionization measurements of the present investigation requires a knowledge of certain cross sections. While a very careful determination has been made of the total scattering cross section,

for a number of substances,[17] these measurements were made with carbon detectors, utilizing the reaction $C^{12}(n, 2n)C^{11}$, which has a 20 MEV threshold. The ion chamber of course has no threshold, and is in addition sensitive to gamma radiation as well as neutrons, so the possibility exists that the beam "seen" by the ion chamber is somewhat different from that "seen" by the carbon detectors, and as a result different cross sections are appropriate.

To test this point, good geometry total scattering cross sections of carbon and copper were measured simultaneously with carbon detectors and with the ionization chambers.[d] The results are given in Table 7, along with certain other cross section measurements.

Table 7 - Good Geometry Total Scattering Cross Sections, as Determined with Carbon Detectors and with Ionization Chambers.

	Simultaneous Determination		Final Values	
	Carbon Detect. m.e.	Ion Chamber m.e.	Carbon Detect. est. error	Ion Chamber m.e. est. error
H			.083 ± .004	.077 ± .011
C	.554 ± .007	.570 ± .008	.550 ± .011	.564 ± .005 ± .011
O			.765 ± .020	.764 ± .015
Cu	2.12 ± .02	2.29 ± .05	2.22 ± .04	2.20 ± .05 ± .05

The columns headed m.e. give the mean error estimated from the agreement between the measurements. The carbon detector final values are from Ref. 17. The ion chamber final values include those of the simultaneous determination along with values determined on two other occasions.

d - The carbon detector measurements were made by Prof A.C. Helmholtz and Mr J. Petersell.

Since the main uncertainty in the ion chamber measurements seemed to lie in uncertainty in the background correction due possibly to non-linear response of the detection system, the computed error is believed to be too small, and an error is estimated based on a 2% error in ϵ_2 and T_0. This is given in the last column of Table 7. The estimated error for the carbon detector values was arrived at in somewhat the same fashion.

It is seen from Table 7 that if any difference exists between the carbon detector and ionization chamber cross sections, it is within present experimental uncertainties. As a result, the cross sections from Ref. 17 will be used in discussing the data from the ionization chamber measurements.

5. Total Ionization Comparisons

From the transition curves corrected for bad geometry attenuation, Figure 7, there can be read off the relative total ionization of the different materials. The same method has been used for some eight different materials. From their relative ionization currents, and

from Eq. (16), there have been computed the values

$$X_C / X_H = 2.19 \pm .06 \text{ (m.e.)}$$

$$X_O / X_H = 2.67 \pm .17 \text{ (m.e.)}$$

Then, using these numbers, the expected relative ionization has been computed, and compared with the observed. The data, and the comparison, is given in Table 8.

Table 8 - Total ionization current relative to carbon, observed and computed, for various materials.

	Carbon	Poly-styrene	Paraf-fin	Water	Oxalic Acid	Lactose	Lucite	Plexi-glas
Aug. 19	1.000	1.238	1.344					
Aug. 23	1.000		1.338				1.191	1.206
Sept. 13	1.000	1.186	1.321				1.196	1.208
Sept. 18	1.000	1.263		1.302	1.124	1.199		
Oct. 11	1.000	1.161	1.335					
Mean observed	1.000	1.212	1.334	1.302	1.124	1.199	1.194	1.207
Computed	1.000	1.19	1.34	1.27	1.12	1.17	1.21	1.21
O - C,%		+1.7	-0.7	+2.3	0.0	+ 2.5	-1.7	0.0

The agreement between the observations and the computed values is probably to be considered satisfactory. The maximum error occurs for water, which is the least well-determined value, consisting of a single point only on the transition curve. The agreement between observations taken at different times is entirely satisfactory, except for polystyrene, where the spread in observed values is much larger than the accuracy of the observations would seem to warrant. No explanation has been found for the spread in the observations.

The calculation was made in the following fashion: If Eq. (16)

is written out for material containing C and H only, and also written out for C alone, and if the ratio of the two equations is taken, there results the equation

$$\frac{X_H}{X_C} = \frac{C_{C1}}{C_{H2}} \frac{I_2}{I_1} - \frac{C_{C2}}{C_{H2}}$$

where the subscript 1 refers to the carbon chamber, and the subscript 2 refers to the C - H chamber, and $C_{ik}=(P_i\ f_i/A_i)_k$, where i = H,C,O, and k = 1,2. Then for I_2/I_1 we use the tabulated value of the relative ion current from table 8, for polystyrene or paraffin, with the appropriate values of f_i/A_i and P_i, and we solve at once for $X_C\ /\ X_H$, getting of course two values. Then, a similar equation is written down for an O - H chamber, and a C - O - H chamber, which now involves the value of $X_C\ /\ X_H$. Using the mean of the two values, and putting in the observed relative ion currents, values are computed for $X_O\ /\ X_H$ for the remaining five substances of Table 8. Then the mean of these values is taken as the provisional value of $X_O\ /X_H$. Then these provisional values of the ratios are used to compute difference equations, giving seven simultaneous, linear equations from which to compute the best correction to the provisional ratios. A least squares solution is made from these seven equations in two unknowns, giving the corrections which, when applied to the provisional values yield the final values stated at the beginning of the present section. The mean errors quoted there are given by the least squares solution from the agreement between the observed and computed values.

Calculation showed that the final values of the X_i ratios were not very sensitive to the energy assumed in calculating the stopping powers P_i, since these enter the calculations only as ratios. For the purposes of this calculation, it was assumed that the average energy of

For the purposes of this calculation, the effective energy of the recoils from hydrogen was taken to be 60 Mev, and the effective secondaries from carbon and oxygen were taken to be 20 Mev protons. These numbers represent attempts to form roughly the averages expressed in Eqn. (10). For hydrogen, the function f_H of that equation is a constant (since, as is pointed out below, the average fractional energy transfer to a proton is $\frac{1}{2}$), but the weight function E_1 of that equation means that the appropriate effective energy is greater than the average energy of the recoils. The presence of heavier particles among the secondaries from carbon and oxygen must bring the effective proton energy down to a somewhat lower value. While the numbers chosen are only estimates, calculation shows that the final values of the X_1 ratios are insensitive to the assumed effective energies, due to the constancy of the stopping powers in this energy region. Values of $\overline{1/S}$ for these energies were taken from Table 3. For lactose and oxalic acid the value of $\overline{1/S}$ was estimated from that of $1/S$ by inspection.

the secondaries from hydrogen is 60 MEV, and the average energy of the secondaries from carbon and oxygen is 20 MEV. So the values of $\frac{L}{S}$ taken from Table 5 for these energies were used. For lactose and oxalic acid the value of $\frac{L}{S}$ was estimated from that of $\frac{l}{S}$ by inspection.

6. Ranges of Secondaries from Carbon

The extrapolation chamber measurements indicated that there are no predominant groups of particles with ranges less than one centimeter. While the extrapolation chamber was unable to carry these observations further, the shallow ion chamber offered the opportunity to extend the investigation of ranges. The ion chamber was set up with the thin foil in the normal, upstream position, and the ionization current was studied as a function of the distance from the chamber of a thin layer of carbon or polystyrene. The current of course decreased steadily as the material was moved away from the chamber. Several groups of particles seemed to be indicated by sharp decreases in the slope of the current curve. The position of these breaks is given in the following table:

Table 9 - Apparent Upper Limit to Groups of Secondaries From Carbon.

distance in cms. of air	1.5	5.5	12
corresponding proton energy, Mev	.85	1.7	2.7
corresponding alpha energy, Mev	1.95	6.7	10.8

The longest of these is seen to correspond well with the first bend in the polystyrene transition curves of Figure 10. The others would not show up in the transition curves, being too close to the origin.

The original curves are not presented here, since as a result of these range measurements, a program has been started for investigating these ranges with a differential chamber, which should give results

superior in accuracy to that obtained with the present shallow chambers.

7. Absolute Neutron Flux Measurements

Since the ionization chambers used in the present investigation allow a determination of the absolute value of the energy flux of the beam, a comparison between flux determined in this manner and flux determined by an entirely independent method should give a check on the validity of the assumptions involved in the interpretation of the ion chamber measurements. This comparison was made by making simultaneous flux determinations with the ion chambers described and with proportional counters. The flux determination with the counters involved the total scattering cross section[17] and the angular distribution of the scattered protons, determined by the same experimental set-up with the proportional counters, from which data the neutron flux can be computed in neutrons /cm^2/sec.^{2} The method has been reported[19].

The ion chamber used in these measurements was made of Plexiglas. Putting the appropriate numerical values into Eq. (16), the flux as measured by a Plexiglas (or Lucite) chamber is given by

$$\phi = 3.\overset{59}{\cancel{64}} \times 10^7 \, I / V \quad \text{Mev/cm}^2\text{/sec}$$

where I is the ion current in micromicroamperes, V is the chamber volume in cm^3, and it has been assumed that the secondaries from a carbon or oxygen nucleus are equivalent to a 20 Mev proton, and the recoil from a hydrogen nucleus is equivalent to a 60 Mev proton, for the purpose of computing stopping powers. (The value $X_H = .0415$ baths was used for reasons given in the final section of the paper.)

The observed current in the Plexiglas chamber was corrected for bad geometry attenuation by assuming that the ionization centroid was at 1.0 cms. The readings on the Zeus output meter were converted to micro-

microamperes by calibrating the meter with a known input voltage, and using the rated values of the grid resistor (of the order of 10^{11} ohms).

Two additional corrections were needed for the ion chamber readings, which were determined by subsequent experiments. The first of these was the beam intensity along the bench, since the ion chamber was mounted 153 cm downstream from the scatterer used for the proportional counters. To investigate this, one ion chamber was used as a monitor on the extreme upstream end of the neutron bench, and the other was moved along the bench, measuring current relative to the monitor. It was found that the beam intensity fell off very nearly as the inverse square of the distance from the Be target. ~~The measurements actually fitted somewhat more closely a $1/r^{2.1}$ power curve, rather than an inverse square curve, though it is not clear that the difference is significant in a statistical sense.~~ Using these measurements, the correction for beam fall-off was 18%.

The second correction determined in a separate experiment was that for recombination. The ionization current was measured (relative to a monitor, as usual) as a function of applied voltage on the ion chamber. These results were then used to compute the saturation current, according to the theory of recombination with columnar ionization developed by Jaffe[8], using the graphs given by Zanstra[7], to simplify the computation. The method consists in plotting $1/i$ against $f(x)$, where i is the observed ion current, x is the field in volts/cm , and $f(x)$ is a function read from Zanstra's graphs, which has been computed from Jaffe's theory. These points should, according to the theory, lie on a straight line which, when extrapolated to the axis of ordinates, gives the reciprocal of the saturation current. Fig. 9 shows this plot for the data of the present ion chambers, for all the experimental points which lay within the range of Zanstra's graphs. This graph gives a saturation current

4% above the

current observed with the operating voltage gradient, 67 volts/cm, which is represented by the point at $f(x) \sim 1.4$. Fig. ~~13~~ 10 shows the same points replotted on a linear voltage scale, including one point which lay outside the range of Zanstra's graphs. It is seen that the computed saturation current seems to fit the data well.

In addition to these corrections needed for the ion chamber measurements, it is necessary to assume an average neutron energy, to convert energy flux into particle flux. For this purpose, the average neutron energy was taken to be 90 Mev, the theoretical value[20].

The actual comparison of the two methods for measuring flux was a series of ten simultaneous measurements. Using all the corrections mentioned for the ion chamber measurements, and using flux values computed from the counter measurements[e], the mean value of the ten ratios of the simultaneous flux determinations came out ~~1.00~~ 1.02 ± .02 (m.e.), where the error is computed from the agreement between the ten values of the ratio. The ~~exact~~ close agreement between the two methods is to be regarded as fortuitous, since neither of the two methods of absolute flux determination is to be considered as certainly free of systematic errors within the computed mean error.

The actual value of the neutron flux was 5×10^5 neutrons/cm^2/sec., in the experiments cited. This indicates a maximum neutron flux of about 2×10^6 for full beam, at a distance of 17.7 meters (58 ft.) from the Be target.

8. Calibration of Monitor for Dosage Measurements

In order to apply the results of the present investigation to biological and medical experimentation, it is desirable to calibrate monitors suitable for use with the extended radiation exposures necessary in biological work. The ion chambers designed for the present work could be used, by "integrating" the exposure, that is to say, reading the instan-

---

[e] These measurements and computations were made by H.F. York, of the Radiation Laboratory.

taneous radiation at regular intervals and estimating the average radiation exposure from this. It is probably more convenient under most conditions to calibrate a conventional, commercial radiation exposure meter. While the choice of monitor depends somewhat on the nature of the biological experiment, one such monitor has been calibrated as a guide to the method.

The commercial chamber calibrated was a 25 r Victoreen chamber. The method was as follows: First, the two cavity chambers used in the present work were placed on the neutron bench, one at the extreme upstream end, and one at about the middle. Then, by reading the ratio of the ion current in the detector to that in the monitor, it was possible to determine exactly the attenuation caused by putting the Victoreen chamber, mounted in a paraffin block, immediately upstream from the detector chamber. In this fashion the cavity chamber and the commercial chamber could be corrected to the same beam value. Then the monitor cavity chamber was removed, and the Victoreen chamber compared to the remaining cavity chamber by taking a series of simultaneous readings.

The cavity chamber material was Lucite. The Victoreen chamber was mounted in a cube of paraffin 15.3 cm on a side. The readings of the Victoreen chamber were corrected for bad geometry attenuation, while the readings of the cavity chamber were corrected for bad geometry attenuation, for beam fall-off along the bench, for attenuation by the Victoreen chamber and its paraffin block, and for recombination. Then, using the experimental value for the ratio of the total ionization of a paraffin chamber and a Lucite chamber, the observed readings in the two were compared, and it was found that the Victoreen chamber read 11.5% high, that is to say, if Q' is the nominal reading in roentgens of the

Victoreen chamber surrounded by an equilibrium thickness of paraffin, then $.87Q_1'$ can be taken to be esu/cc under the conditions of the present experiment.

To make use of this result, numerical values must be put into Eq. (20). Using the formula for wet tissue stated in the discussion of ranges, for the purpose of computing stopping powers and as usual assuming that the secondaries from a carbon and oxygen nucleus may be taken to be 20 Mev protons, while the recoil from a hydrogen nucleus may be taken as a 60 Mev proton, the tissue dose is computed from Eq. (20) as

$E_v = 1.31 Q_1$ rep, for a paraffin cavity chamber

[illegible] Lucite or Plexiglas chamber

where Q_1 is the measured accumulated charge in the chamber in question, in esu/cc. Then for the paraffin-enclosed 25 r Victoreen chamber calibrated,

$$E_v = 1.31 \times .87\, Q_1' = 1.14\, Q_1' \text{ rep.}$$

where Q_1' is the nominal reading in roentgens. It should be emphasized that the last equation applies only to the one chamber calibrated, and only to tissue of the assumed composition.

The intensity of the radiation dosage measured in these experiments was about 6.1 rep/hr. This would mean a maximum dosage of about 30 rep/hr at the center of the neutron bench for the maximum neutron beam available at the present time. Assuming an inverse square beam, this would give about 1150 rep/hr just outside the cyclotron tank wall.

V - DISCUSSION OF THE EXPERIMENTAL RESULTS

1. The energy transfer coefficients X_H, X_C, and X_O.

It was pointed out in the discussion following Eq. (14) that one of the four unknowns, X_C, X_O, X_H, and Φ must be determined by another method due just to the fact that Eq. (14) is an homogeneous equation. The first two cannot at the present time be measured in any other fashion. The energy flux Φ could be ~~taken~~ computed from the proportional counter measurements on angular distribution of scattered protons as discussed above, but the result then would contain not only the uncertainties of that experiment, but also the uncertainty in the estimate of the average neutron energy, since that experiment gives particle flux, and Φ is energy flux. We are left then with the quantity X_H, the numerical value of which can in fact be estimated with reasonable accuracy. Since a neutron-proton collision is necessarily elastic and produces always one ionizing particle, X_H must be given by the product of the average fractional energy transfer from a neutron to a proton, times the total scattering cross section of a hydrogen nucleus.

If the n-p scattering is isotropic in center-of-mass of coordinates, the average fractional energy transfer must be exactly $\frac{1}{2}$, a result which follows from the conservation of momentum. While it has not yet been finally decided whether this scattering is exactly isotropic for 100 Mev neutrons, this assumption fits fairly well the meager experimental data now available. (The angular distribution of the recoil protons is being studied with the cloud chamber by Dr. Wilson Powell and his collaborators, and with proportional counters by H. F. York and his collaborators[19]). Thus it will be assumed that the average fractional energy transfer from a neutron in the beam of the 184-inch cyclotron to a proton is $\frac{1}{2}$. If at some later time it is found that the scattering is not isotropic, then the numerical results will have to

be revised, but it seems unlikely at the present time that this figure will be changed by as much as 10%.

The best value of the total scattering cross section for hydrogen is at present .083 barns[17]. The reason for adopting this value, rather than the slightly lower value determined with the ion chambers, is given in the discussion of the cross section measurements. So now the relevant experimental data may be summarized as follows:

$$X_H = \tfrac{1}{2}\,(.083 \pm .004),\quad X_C/X_H = 2.19 \pm .06,\quad X_O/X_H = 2.67 \pm .17$$

From these may be calculated

$$X_C = .091 \pm .004 \text{ barns} \qquad X_O = .111 \pm .009 \text{ barns}$$

The errors quoted represent mean errors calculated from the agreement of the data, except for X_H, where the experimental error was increased (by the original authors) to take account of possible systematic errors. Thus the final values of X_C and X_O show experimental mean errors of 4 and 8%, respectively. If now we assign to the average energy per ion pair, to the average relative stopping powers, and to the average fractional n-p energy transfer the respective "uncertainties" of 5, 5, and 10%, and if we propagate these as if they were true mean errors, we get a final estimated "uncertainty" of about 15% in both X_C and X_O.

An accurate interpretation of these numbers involves a certain amount of theoretical information not now available. The qualitative discussion which follows will be revised at such a time as that information becomes available.

The quantity X_C was defined as

$$X_C = \overline{\gamma_C\, k_C\, \sigma_C}$$

where γ_C is the average energy of an ionizing secondary, expressed as a fraction of the average neutron energy, k_C is the average number of ionizing secondaries per collision, σ_C is the cross section for collison with production of one or more ionizing particles, and the bar signifies "average over the

energy of the beam weighted with the energy". [redacted] As has been mentioned above, for the entire energy spectrum of the beam, the carbon neutron [redacted] λ is appreciably less than the radius, and as a result it may be expected that the collision cross section will be approximately the geometrical cross section for all the neutrons, independent of energy. So it will not be a bad approximation to remove σ_c from the integral indicated by the bar, and write

$$\overline{\lambda_c k_c} = .089\, \sigma_c$$

To get the appropriate cross section for use in this equation, it is necessary to subtract from the total scattering cross section the sum of all the cross sections for processes which do not result in at least one ionizing particle.

Now it can be shown that for a spherical nucleus which completely absorbs all incident particles which collide within the radius R, the total scattering cross section is $2\pi R^2$, provided $R \gg \lambda$, the wave length of the incident particles. This is seen [redacted] to be plausible, by analogy with optical diffraction by a circular reflecting disk, in which case the forward and backward diffraction patterns are identical (Babinet's principle).

Since in the present energy region every neutron which collides with a carbon nucleus, that is to say, which approaches the nucleus within the range of the nuclear forces, can be expected to undergo an inelastic collision, the cross section for elastic scattering must be just $\frac{1}{2}$ the total scattering cross section. Besides the elastic scattering, there are various other processes which may take place without production of ionizing particles, such as (n, n γ), (n, 2n), (n, 3n), etc. Since the reaction C^{12} (n, 2n) C^{11} has a radioactive end product, it has been possible to determine that the cross section for this reaction is .025 $\pm$ .005 barns[19].

The cross section for the other processes which do not produce ionizing secondaries is not known. Thus the estimate of the cross section for collision with production of one or more ionizing secondaries is

$$\sigma_C = \tfrac{1}{2}(.55) - .025 = .25 \text{ barns}$$

which is 45% of the total scattering cross section. It is assumed that a similar cross section for oxygen is

$$\sigma_O = \text{[illegible]} \times .765 = .348 \text{ barns}$$

Then using these cross sections, and taking the average neutron energy to be 90 Mev, we calculate for the average energy of the secondaries from a single collision

$$C = 33 \text{ Mev; and } O = 29 \text{ Mev.}$$

If theoretical calculations to be made indicate that the (n, n α) and (n, 3n) cross sections are appreciable, these estimates will have to be revised upwards, perhaps as much as 10% (which is the amount of the (n,2n) contribution). [illegible]

It is not possible at the present time to estimate the average number of ionizing particles per collision with any accuracy, but a guess would place it between 1 and 2. This guess is based upon the cloud chamber data (unpublished) which indicates that the 2-, 3-, and 4-pronged stars resulting from neutron collisions are roughly in the ratio 4:2:1. This would indicate that the average energy of all the secondaries from a neutron collision with a carbon nucleus is between 32 and 16 Mev, probably nearer the former. It is interesting that this checks qualitatively with the "ionization centroid", that is, the energy of a proton whose range is the effective distance from which particles reach the ion chamber, which for carbon was found above to be 27 Mev.

bring out neutrons per " " unit.